JACS
JOURNAL OF THE AMERICAN CHEMICAL SOCIETY
Perspective
pubs.acs.org/JACS

Kinetic Profiling of Catalytic Organic Reactions as a Mechanistic Tool

Donna G. Blackmond*

Department of Chemistry, The Scripps Research Institute, La Jolla, California 92037 United States

ABSTRACT: The use of modern kinetic tools to obtain virtually continuous reaction progress data over the course of a catalytic reaction opens up a vista that provides mechanistic insights into both simple and complex catalytic networks. Reaction profiles offer a rate/concentration scan that tells the story of a batch reaction time course in a qualitative "fingerprinting" manner as well as in quantitative detail. Reaction progress experiments may be mathematically designed to elucidate catalytic rate laws from only a fraction of the number of experiments required in classical kinetic measurements. The information gained from kinetic profiles provides clues to direct further mechanistic analysis by other approaches. Examples from a variety of catalytic reactions spanning two decades of the author's work help to delineate nuances on a central mechanistic theme.

INTRODUCTION

Mechanistic studies of multistep catalytic organic reactions such as the general network of a coupling reaction **A** + **B** → **C** shown in Scheme 1 focus on elucidating factors that control product distribution or affect catalyst turnover. Such investigations often lead to attempts to characterize catalytic intermediates (such as **cat**, **I**, and **II** in Scheme 1) either by isolation, spectroscopic identification, or computational modeling. Researchers may then turn to kinetic analysis late in the game to corroborate a mechanistic proposal based on such proposed intermediates. This order of events can be problematic, however, in many catalytic systems where intermediate species may be too fleeting within the cycle, too low in concentration to observe spectroscopically, or too unstable for isolation. In such cases, analysis of the global kinetics of the working catalytic cycle provides the most direct information about the nature of kinetically relevant intermediates, the catalyst resting state, and the turnover-limiting step. In fact, it may be argued that global kinetic analysis provides a direct window onto the steady-state catalytic cycle in *all* cases—even in examples where species have been identified by other means. In any case, the relevance of an isolated intermediate to the catalytic cycle is only confirmed by demonstration of its consistency with the reaction kinetics. Why, then, is kinetic analysis not the first act in a mechanistic study rather than, as is more often the case, the last?

Scheme 1. General Cycle for Steady-State Catalytic Reaction A + B → C[a]

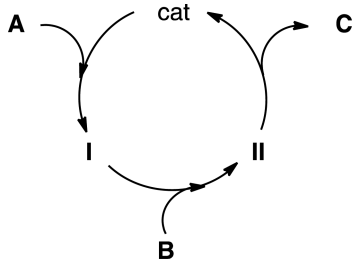

[a]All steps may be reversible.

Experimental kinetic studies are often regarded by synthetic organic chemists as being too tedious, tough, and time-consuming to become standard practice for the initial report of a new reaction. Certainly the repetitive nature of initial rate measurements or pseudo-first-order methods using artificially constructed concentration conditions (e.g., holding one substrate concentration constant at a 10-fold excess while measuring the rate dependence on a second substrate's concentration) may evoke memories of dull undergraduate laboratory sessions, where the task of compiling tables of log values feels far removed indeed from the excitement of encountering a new organic transformation. Classical kinetic methods have historically made us "slaves to the straight line."[1] By contrast, with modern experimental and computational tools we can monitor reaction progress instantaneously and virtually continuously, with rapid and facile data manipulation that reconnects us with the thrill of the chemistry itself.

Monitoring temporal reaction progress gives us a way of looking inside a reaction to tell the full story of the catalytic mechanism, where, in comparison, it might be said that classical kinetic methods provide merely a snapshot. Reaction progress kinetics of a catalytic network is a narrative that shifts as the story unfolds: as the substrate concentrations decrease over the course of a catalytic reaction, the relative importance of different intermediate species—the different characters in the story—changes. The sensitivity and accuracy of in situ measurements, together with advances in computational methods for describing intermediates, allow "character development" in more compelling detail than ever before. Indeed these new methods cry out for a renaissance to unfold in organic reaction mechanistic analysis. What would the champions of physical organic chemistry from its heyday in the mid-20th century have given for access to such tools?

Reaction progress kinetic analysis (RPKA) is a methodology developed to extract maximum information from a minimal number of experiments designed to be mathematically independent, via graphical manipulations of time course data.[2] In addition, the reaction profile itself may serve as a mechanistic fingerprint not only for straightforward kinetic

Received: June 5, 2015
Published: August 18, 2015

DOI: 10.1021/jacs.5b05841
J. Am. Chem. Soc. 2015, 137, 10852−10866

scenarios of reactions following steps such as shown in Scheme 1 but also for more complex cases. Once the outline of the reaction's story is sketched by kinetic analysis, further plot details may then be elaborated by employing other mechanistic approaches suggested by the findings of the kinetic analysis. For example, if a reaction following Scheme 1 is inferred by RPKA to exhibit turnover-limiting addition of **A** to **cat**, it is unlikely to be useful to devote effort to isolating either intermediate **I** or **II**, because the kinetics predict that they will be present in fleeting concentrations compared to **cat**. Conversely, if the reaction exhibits first-order kinetics in [**B**], experiments aimed at identifying species **I** might be valuable, since such kinetics suggest that the resting state lies at species **I**. Thus, the kinetic analysis provides clues about where to look and what to look for in further mechanistic experiments using other tools; a good reason to carry out the kinetics first!

This review considers a number of examples of catalytic reactions studied in our laboratories over the past 20 years, mainly in liquid or multiphase reactions of pharmaceutical interest carried out in batch reactors, highlighting cases where RPKA has helped to streamline our mechanistic investigations. The examples are divided into seven themes, each summarized with a "take-home message",[1] designed to highlight the power of kinetic profiling to elucidate mechanistic detail even as layers of increasing complexity supplement the simple catalytic network of Scheme 1. We finish with a step-by-step protocol illustrating how to carry out this kinetic analysis.

RESULTS AND DISCUSSION

Experimental Methods and Definitions. Kinetic profiling requires that a correlation be established between reaction rate and some property that is measured by the monitoring tool. The examples discussed in this work employ reaction calorimetry and FTIR spectroscopy. Reaction calorimetry correlates the heat released or consumed in a reaction with reaction rate, as shown in eq 1a, with rate being directly proportional to the heat flow of the reaction. Integration of the heat flow curve gives fraction conversion as in eq 1b.

$$\dot{q} = \Delta H_{rxn} \cdot V \cdot r \tag{1a}$$

$$x = \frac{\int_{t_0}^{t_x} \dot{q}\,dt}{\int_{t_0}^{t_f} \dot{q}\,dt} \tag{1b}$$

where $\dot{q}$ = reaction heat flow (energy/time); ΔH_{rxn} = heat of reaction (energy/mol); V = reaction volume; r = reaction rate (mol/volume/time); x = fractional heat flow; and t_0 and t_f = reaction start and end time points.

For a given reaction, the fractional heat flow may be equated with fraction conversion of the limiting substrate, assumed here to be [**A**], by eq 2:

$$[\mathbf{A}] = [\mathbf{A}]_0(1 - x) \tag{2}$$

Most common methods for monitoring reaction progress do not correlate directly with reaction rate, but instead monitor a property that is proportional to concentration, such as spectroscopic absorbance for systems following Beer's Law as in eq 3a. FTIR spectroscopy is one of the most commonly used tools for monitoring concentration. Reaction rate is obtained by taking the derivative of the concentration as in eq 3b.

$$\text{Abs} = \varepsilon \cdot b \cdot [\mathbf{A}] \tag{3a}$$

$$r = -\frac{d[\mathbf{A}]}{dt} \tag{3b}$$

where Abs = absorbance (unitless); ε = molar absorptivity (volume/mol/distance); and b = path length (distance).

RPKA relies on the relationship between substrates **A** and **B** that is given by the reaction stoichiometry in a catalytic network such as Scheme 1. The key parameter is one called "excess" [**xs**], defined as the *difference* between the initial concentrations of substrates **A** and **B** as in eq 4. Each time one molecule of **A** is consumed in the reaction, one molecule of **B** is consumed as well; the stoichiometry of the reaction of Scheme 1 thus dictates that their difference in concentration remains the same over the course of the reaction. Hence [**xs**] is a constant, with units of concentration, that allows [**B**] to be calculated from [**A**] or vice versa, thus reducing the two-substrate problem of Scheme 1 to a one-substrate problem.

$$[\mathbf{xs}] = [\mathbf{B}]_0 - [\mathbf{A}]_0 = [\mathbf{B}] - [\mathbf{A}] \tag{4}$$

With these definitions in hand and armed with in situ tools capable of measuring kinetic profiles of reaction rate or concentration over the course of the reaction, we turn to a range of examples to illustrate seven themes encompassing the broad range of mechanistic information that becomes accessible through the use of kinetic profiling and RPKA.

Theme 1: Zero-Order Kinetics in One [Substrate]: Is It [A] or Is It [B]? Many catalytic reactions following the simple mechanism shown in Scheme 1 may be described by overall first-order kinetics, with one of the substrates exhibiting zero-order kinetics for one of two reasons: (1) addition of **A** to the catalyst with **B** adding subsequent to the turnover-limiting step; or (2) binding of **A** to the catalyst to give saturation in an intermediate that then reacts with **B** in the turnover-limiting step. In the former case, the reaction is first order in [**A**] and zero order in [**B**]; these dependences are reversed in the latter case. Differences in the kinetic profiles act as "fingerprints" to provide compelling evidence to distinguish each case.

To illustrate kinetic profiling in this example, we choose two Pd-catalyzed coupling reactions shown in Scheme 2. These

Scheme 2. General Scheme for Reactions of ArX (1a–b) with Nu (2a–b) Catalyzed by Pd Complexes (3a–b)

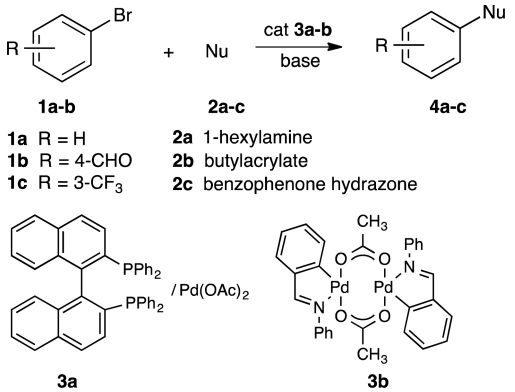

reactions follow the general mechanism of oxidative addition of an aryl halide (**A** = ArX, **1a**, or **1b**) to a catalyst to form intermediate **I** followed by addition of a nucleophile (**B** = primary amine **2a** or olefin **2b**) and reductive elimination of the product **C** from intermediate **II** to regenerate **cat** and complete the cycle. Table 1 shows the conditions for four reactions, two

DOI: 10.1021/jacs.5b05841
J. Am. Chem. Soc. 2015, 137, 10852–10866

for each set of substrates, in each case carried out at two different values of the parameter "excess" [**xs**] defined in eq 4.

Table 1. Conditions of Reactions of Scheme 2 Corresponding to the Kinetic Profiles Given in Figures 1 and 2

entry	ArX, Nu	cat	[ArX] (mM)	[Nu] (mM)	[**xs**] (mM)	[cat]	ref
1[a]	**1a**, **2a**	**3a**	293	405	112	6	3
2[a]	**1a**, **2a**	**3a**	101	405	304	6	3
3[b]	**1b**, **2b**	**3b**	200	200	80	0.02	4
4[b]	**1b**, **2b**	**3b**	80	200	120	0.02	4

[a]5 mL volume; toluene, 1.2 equiv NaO^{t}Bu, 70 °C. [b]500 mL volume; DMAc, 1.5 equiv NaOAc, 140 °C.

For reactions carried out under synthetically relevant conditions, the concentrations of both substrates **A** and **B** change continuously over the course of the reaction. Because the parameter [**xs**] gives us the relationship between the two, we need to only measure one, either [**A**] or [**B**], in order to know both. Where classical kinetic analysis requires two complete sets of experiments to determine the reaction orders in [**A**] and [**B**] (holding one constant in each set while varying the other), RPKA extracts the same information—reaction orders in two substrates—in just two experiments carried out at different values of [**xs**]. This is illustrated in Figure 1. Figure 1a,b plots data for the amination reaction of entries 1 and 2 of Table 1 as calorimetric heat flow vs time in Figure 1a and as reaction rate vs [**ArX**] or [**A**] in Figure 1b.[3]

The data in Figure 1a show an exponential decay of [substrate], implying overall first-order kinetics; but the question is first order in which substrate, [**A**] or [**B**]? When these data are replotted as rate (in mM/min) vs [ArX], or [**A**],[2] as in Figure 1b, we obtain linear plots for two reactions that exhibit different concentrations of amine **2a** (substrate **B**) at any given [ArX] (**1a**) that overlay one another and pass through the origin. From this we deduce: (a) the reaction is first order in [**A**] (or [**1a**]), and (b) the reaction is zero order in [**B**] (or [**2a**]). This gives the rate law of eq 5, which is consistent with addition of **A** as the turnover-limiting step and species **cat** as the resting state in the lexicon of Scheme 1. Figure 1b represents a "graphical rate equation," where the *y*-axis is the left side of eq 5 and the *x*-axis is the variable [**A**] on the right side of eq 5.

$$\text{rate} = k\cdot[\mathbf{A}] \tag{5}$$

Kinetic profiles of the reaction of **1b** and **2b** (as **A** and **B**) from Scheme 2 and Table 1 (entries 3 and 4) at two different values of [**xs**] are shown in Figure 1, right.[4] Reaction rate vs time is shown in Figure 1c. The rate profiles in this case appear to be more complex than in the reaction of **1a** and **1b**, with a monotonically decreasing rate that exhibits a "bump" at higher conversion (marked at the arrows in Figure 1c). When replotted as reaction rate vs [ArX] as shown in Figure 1d, however, the rate curves for the two reactions are linear until

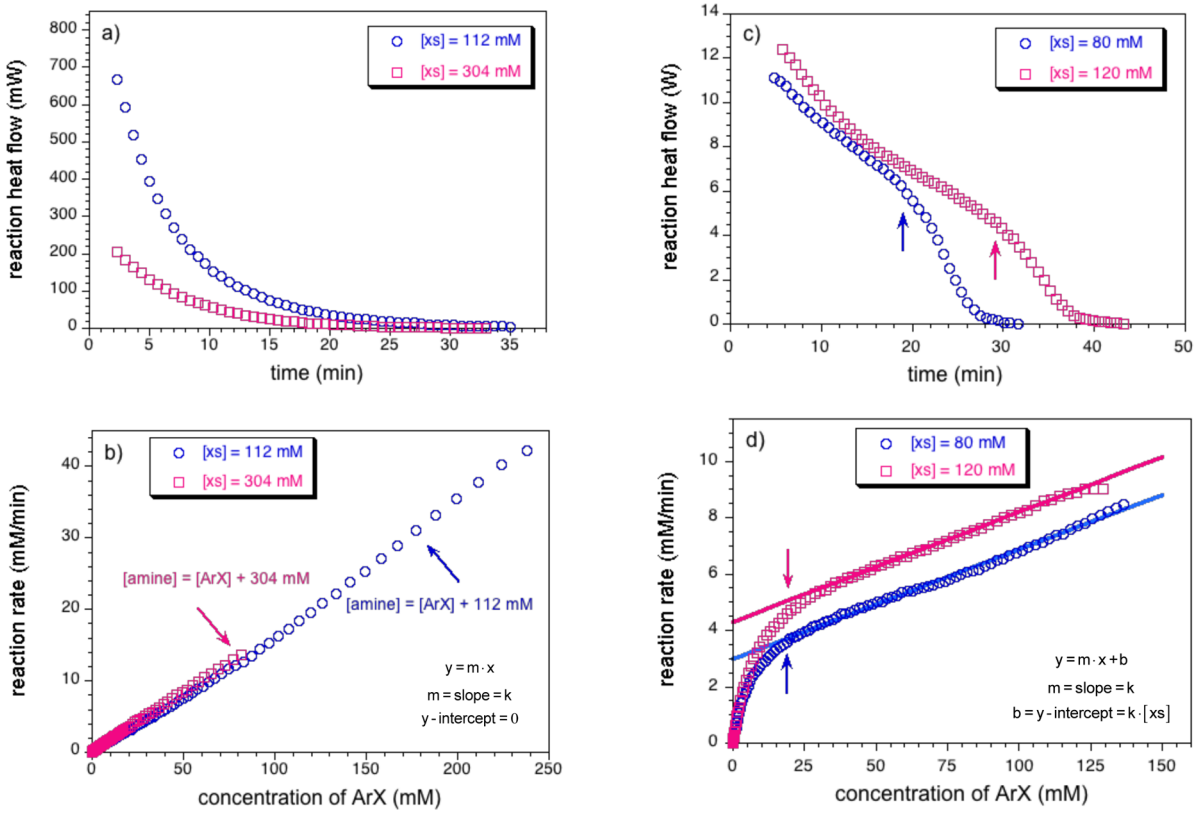

Figure 1. Kinetic profiles from reaction shown in Scheme 2. Left: Table 1, entries 1 and 2.[3] (a) Rate vs time; (b) data from part (a) plotted as rate vs [ArX], [**1a**]. As described in the text, the linear behavior, overlay between the two curves, and *y*-intercept = 0 indicates that the reaction is first order in [**1a**] and zero order in [amine], [**2a**]. Right: Table 1, entries 3 and 4.[4] (a) Rate vs time; b) data from part (a) plotted as rate vs [ArX], [**1b**]. As described in the text, the linear, identical slopes with nonzero *y*-intercepts related to the value of [**xs**] indicate zero-order kinetics in [**1b**] and first-order kinetics in [amine], [**2b**].

DOI: 10.1021/jacs.5b05841
J. Am. Chem. Soc. 2015, 137, 10852−10866

high conversion, exhibiting offset straight lines of identical slope that do not intersect the origin. The "bump" that was visible in the temporal rate curves is observed where rate deviates from linear behavior at the end of the reaction.

The kinetic plots of Figure 1d may be rationalized by considering the definition of [**xs**]. Solving for **B** in eq 4 gives eq 6. If the reaction in this case is first order in [**B**] instead of [**A**] as in the previous example, then the rate may be written in terms of [**A**] as in eq 7.

$$[\mathbf{B}] = [\mathbf{A}] + [\mathbf{xs}] \tag{6}$$

$$\text{rate} = k\cdot[\mathbf{B}] = k\cdot[\mathbf{A}] + k\cdot[\mathbf{xs}] \tag{7}$$

This is the equation of a straight line with a nonzero *y*-intercept, $y = mx + b$, with slope = k and *y*-intercept = $k\cdot[\mathbf{xs}]$. Figure 1d represents the "graphical rate equation" given by eq 7. The slope of the linear portion of both curves in Figure 1d gives $k = 0.039\ \text{min}^{-1}$. The *y*-intercepts are 4.31 and 2.97 mM/min, in good agreement with the values 4.68 and 3.12 M/min calculated from the slope multiplied by the experimental [**xs**] values.

A reaction that exhibits zero-order kinetics in the concentration of substrate **A** and first-order kinetics in [**B**] in a mechanism following that of Scheme 1 may be rationalized by suggesting that intermediate **I** is the catalyst resting state, i.e., the cycle is saturated in species **I**, and that addition of **B** is turnover-limiting. In cases where **A** is the limiting reactant, the reaction will follow overall first-order kinetics (in [**B**]) until the concentration of **A** approaches zero, at which point the rate necessarily plunges precipitously to zero (because a reaction cannot have a nonzero rate with zero substrate concentration), producing the "bumps" in Figure 1c and the corresponding bends in Figure 1d. The catalyst resting state shifts accordingly back to [**cat**] when [**A**] approaches zero.

Take-Home Message. The data plotted in Figure 1 describe two reactions that each exhibit overall first-order kinetics, but the distinct features of their kinetic profiles may be used as diagnostic fingerprints for determining which concentration—substrate **A** or substrate **B** in the lexicon of Scheme 1—is responsible for the rate dependence in each case as well as defining the catalyst resting state. This example may be generalized with the following two rules for plots of rate vs [limiting substrate] at two values of [**xs**]: (i) plots that are linear, exhibit overlay, and pass through the origin are fingerprints for reactions that are first order in the concentration of the limiting substrate and zero order in the other (excess) substrate's concentration; (ii) plots that give offset straight lines with nonzero intercept are fingerprints for a reaction that is zero order in the concentration of the limiting substrate (plotted as the *x*-axis) and first order in the other (excess) substrate's concentration. In each case, designing two separate reactions carried out at different [**xs**] is sufficient to determine concentration dependences of two substrates **A** and **B**.

A further take-home message from this example is to note the rich features that may be observed in the kinetic data when reaction time is removed from the picture, as in Figure 1b,d. While it may be argued that for the simpler first-order case, the exponential decay of rate vs time plot of Figure 1a, would suffice to provide the same information as the graphical rate equation of Figure 1b, the more complex case of Figure 1c, is more difficult to glean from time courses of either rate or concentration. The features of this reaction, saturation kinetics, and a shifting catalyst resting state are clarified in the graphical rate equation of Figure 1d.

Theme 2: Rate Profiles As Diagnostics for Comparing the Turnover-Limiting Step in a Series of Reactions. Many reactions in a particular class follow similar mechanistic steps but exhibit differences in turnover-limiting step and catalyst resting state. The Pd-catalyzed coupling reactions examined in Theme 1 provide one example. Another case that is a classic theme is the reaction between carbonyl compounds and electrophiles catalyzed by aminocatalysts, as shown in Scheme 3. A wide variety of different transformations utilizing different catalysts have been reported since the turn of the century, which saw a resurgence in "organocatalysis" following publication of the proline-catalyzed intermolecular aldol reaction by Barbas and co-workers[5] and Macmillan's Diels–Alder reaction catalyzed by oxazolidinone salts.[6] Such reactions following an enamine mechanism include aldol, aminoxylation, amination, halogenations, selenylations, and Michael additions to nitroalkenes and enones, among others.[7] Surprisingly, with such a broad substrate scope under this general mechanism established, few kinetic studies had been carried out prior to the detailed work of our group. Reactions of Scheme 3 following an enamine mechanism may be couched in terms of the general network of Scheme 1, with **cat** as the organocatalyst **7a**–**7d**, the enamine intermediate as **I**, and a "downstream intermediate species" **II** containing both the carbonyl compound **5** and the electrophile **6** associated with the catalyst. Much information may be extracted simply from comparison of the kinetic profiles of these reactions, even without the further manipulations shown in the previous example. Differences between these profiles are fingerprints of features of each reaction, providing information about the rate-limiting step and the catalyst resting state. In each case, kinetic profiles are shown as both rate/time and conversion/time plots, illustrating and comparing data from the two types of experimental methods described earlier.

Table 2 lists conditions for five different reactions between different carbonyl compounds and electrophile for which we have monitored reaction progress kinetic profiles. Figure 2 shows kinetic profiles for the three reactions of entries 1–3 in Table 2, with rate vs time on the left and conversion vs time on the right.

The kinetic profile plotted in Figure 2, top, of the α-chlorination of isovaleraldehyde **5a** with the quinone chlorinating agent **6a** catalyzed by the oxazolidinone **7a**[8] shows that the reaction clearly follows first-order kinetics.[9] In analogy to the Pd-catalyzed amination reaction shown in Figure 1a, we can propose that intermediate **I** (enamine) formation is turnover-limiting and that the catalyst resting state is **cat** (**7a**). This was later confirmed by different [**xs**] experiments.[9b]

By contrast, the plot of the aldol reaction in Figure 2, middle,[10] exhibits positive-order kinetics that are not strictly first order, as may be seen by comparison with the conversion vs time curve simulated for first-order kinetics in gray. Our work has shown[10a] that this type of profile is characteristic of a reaction where the resting state shifts over the course of the reaction, partitioning between **cat** and **I**. This was confirmed in more detailed different [**xs**] experiments. Thus, the system exhibits saturation kinetics but is not fully saturated in [**I**], as it was in the previous example of Figure 1b,d. In this case both substrates **A** and **B** contribute to the rate. At higher concentrations of **A**, the acetone substrate **5b**, the resting state shifts further toward **I**. Noninteger reaction orders serve as

DOI: 10.1021/jacs.5b05841
J. Am. Chem. Soc. 2015, 137, 10852–10866

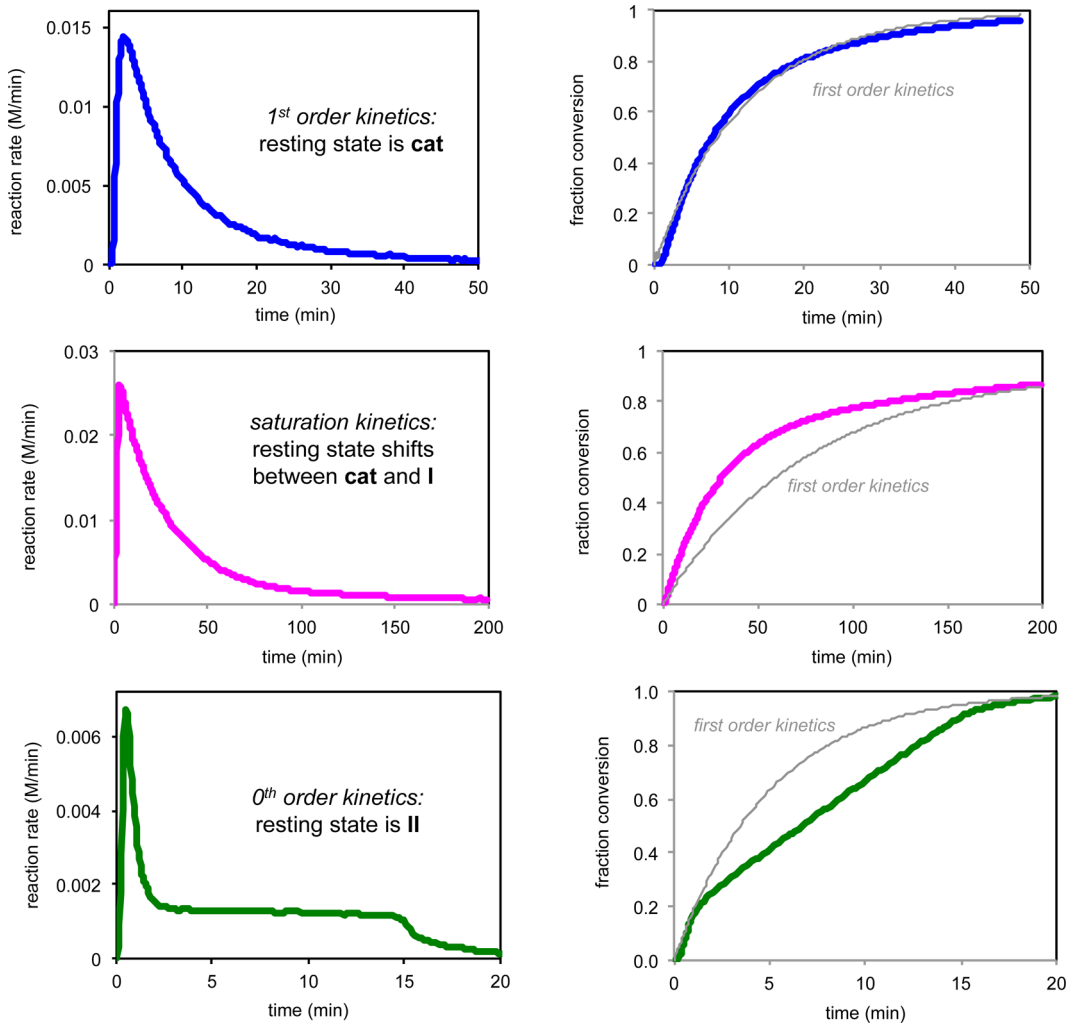

Figure 2. Kinetic profiles of the organocatalyzed reactions shown in Scheme 3, entries 1−3. Left: rate vs time; Right: conversion vs time. Top: entry 1, Table 2[9] (substrates **5a** and **6a**, catalyst **7a**); Middle: entry 2, Table 2[10] (substrates **5b** and **6b**, catalyst **7b**); Bottom: entry 3, Table 2[11] (substrates **5a** and **6c**, catalyst **7c**). Catalytic resting state in each case refers to the general cycle for **A** + **B** → **C** shown in Scheme 1, where **A** = **5a−c** and **B** = **6a−e**. Simulated first-order fits to conversion vs time are shown in gray on the right side plots.

a shorthand to describe such a case.[10a] The reaction exhibits less than first order in both substrates [**5b**] and [**6b**].

Figure 2, bottom, shows a further example of the same mechanistic steps, in this case in the selenylation of isovaleraldehyde **5a** with **6c** catalyzed by the diarylprolinol ether catalyst **7c**.[11,12] This kinetic profile exhibits two characteristic regions, a rapid initial rate of positive order followed by an extended period of zero-order kinetics. Investigations of this and several other reactions catalyzed by **7c** elucidated the origin of these two regimes: the rapid initial rate is attributed to the nonsteady-state buildup of intermediate **II** that contains both substrates **A** and **B**; the slower, zero-order regime is due to the turnover-limiting reaction of this species. In the lexicon of Scheme 1, the resting state is intermediate **II**, which in the reaction of Figure 3c corresponds to the product enamine species formed after selenylation of the isovaleraldehyde enamine. Detailed in situ NMR studies allowed characterization of this intermediate and elucidated its role[11] in solvent-sensitive enantioselectivity.[12b]

Take-Home Message. The distinctly different kinetic profiles in the cases shown in Figure 2 may all be rationalized by the mechanism in Scheme 1 simply by shifting the turnover-limiting step from one intermediate to another. Casual inspection of raw kinetic data can provide a good preliminary picture of the nature of the reaction network. In each case these

Scheme 3. General Scheme for Reactions of Carbonyl Compounds (5a−e) with Electrophiles, E (6a−e), Catalyzed by Organocatalysts (7a−d)[a]

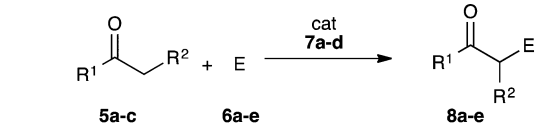

5a R_1 = H, R_2 = $CH(CH_3)_2$
5b R_1 = CH_3, R_2 = H
5c R_1 = H, R_2 = CH_3

6a 2,3,4,5,6,6-hexachlorocyclohexa-2,4-dienone
6b 2-Cl-benzaldehyde
6c Ph-Se-phthalimide
6d DEAD
6e PhNO

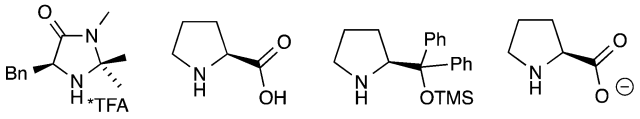

7a **7b** **7c** **7d**

[a]See Table 2.

DOI: 10.1021/jacs.5b05841
J. Am. Chem. Soc. 2015, 137, 10852−10866

Table 2. Reactions of Scheme 3[a]

entry	5	$[5]_0$ (M)	E	$[E]_0$ (M)	cat	[cat] (M)	ref.
1[b]	**5a**	0.21	**6a**	0.25	**7a**	0.02	9
2[c]	**5b**	1.0	**6b**	1.0	**7b**	0.1	10
3[d]	**5a**	0.075	**6c**	0.025	**7c**	0.0025	11
4[e]	**5c**	1.5	**6d**	0.5	**7d**	0.035	13
5[f]	**5c**	2.1	**6e**	0.31	**7b**	0.07	14

[a]All reactions carried out in Omnical reaction microcalorimeter. [b]V = 2.9 mL; T = 15 °C; $CHCl_3$. [c]V = 5 mL; 0.2 M H_2O; T = 25 °C; DMSO. [d]V = 8 mL; T = 25 °C; toluene. [e]V = 5 mL; T = 5 °C; $CHCl_3$. [f]V = 5 mL; T = 25 °C; $CHCl_3$.

profiles provided the first clues that aided in the design of further experiments, which in turn fully elucidated the mechanistic features peculiar to each reaction.

Theme 3: Complex Kinetics Requiring Additional Steps in the Mechanism of Scheme 1. In many cases of catalytic cycles following that of Scheme 1, the main reaction may be accompanied by other reactions that occur off-cycle, connected to the main reaction network in some way. Possibilities include catalyst activation and deactivation, product inhibition or acceleration, and the development of reservoirs of inactive catalyst species. In such cases additional steps must be added to the mechanism of Scheme 1 to explain fully the experimental observations, and in many of these cases, we find that the kinetic profile can be enlisted as a fingerprint to provide valuable clues about the added complexity of the network.

Two such examples in enamine-based organocatalysis according to Scheme 3 led to the unusual kinetic profiles shown in Figures 3 and 4, taken from the α-amination[13] and α-aminoxylation[14] reactions of entries 4 and 5 of Table 2. In Figure 3, a kinetic profile reminiscent in some respects of the selenylation reaction in Figure 2 (bottom) was obtained. In this case, however, the rapid initial rate was followed by an extended period of close to zero order but slightly *rising* rate, culminating in a final rise and rapid dropoff at the end of the reaction. It is also interesting to note that this rising rate is more difficult to discern from the conversion vs time plot (Figure 3b), appearing as a slight change in slope near the end of the reaction.

The reaction profile depicted in Figure 4, from Table 2, entry 5, is even more strikingly unusual, with rate *increasing* monotonically with time and again exhibiting a precipitous dropoff at the end of the reaction. Considering that the substrate concentration is decreasing over this time course, even as the rate increases, these cases lead to the unusual conclusion of negative-order kinetics in substrate. Can simple modifications to the reaction network of Scheme 1 rationalize these unusual observations?

Indeed, in both cases presented in Figures 3 and 4, we were able to propose simple reactions connected to the network of Scheme 1 that fully rationalized the experimental observations and were in turn corroborated by other mechanistic studies. Scheme 4 presents these mechanistic proposals in the lexicon of Scheme 1. The α-amination reaction of Figure 3 and Table 2, entry 4, the rapid initial nonsteady-state reaction rate decreased as increasing amounts of the catalyst are siphoned away into an off-cycle equilibrium due to the reversible reaction of electrophile **6d** with catalyst **7d** to form a stable triazane complex, noted as **III** in Scheme 4a.[13] The rate acceleration observed toward the end of the reaction in Figure 4 occurs when the decreasing concentration of **6d** ultimately causes the off-cycle equilibrium to shift, releasing **B** (**6d**) and **cat** (**7d**) back to the cycle.

In the aminoxylation reaction of Figure 4 and Table 2, entry 5, it was found that the reaction product helps to catalyze the rate of enamine formation, which is the turnover-limiting step in this case.[14] Because the amount of product is increasing throughout the reaction, the rate continues to rise until the final turnovers. The product thus serves as a continuous feed of an accelerating additive in the reaction (Scheme 4b).

Take-Home Message. The examples of Figure 4 depicted in Scheme 4 demonstrate that it may not be necessary to invoke entirely new mechanistic proposals to rationalize even highly unusual kinetic profiles. These examples are explained by addition of simple reactions coupled to the general mechanistic framework of Scheme 1.

Theme 4: Probing Catalyst Robustness. Most kinetic studies of catalytic reactions assume that the concentration of catalyst in the active catalyst cycle remains constant over the course of the reaction and is equal to the total catalyst employed. Indeed, a constant catalyst concentration is a prerequisite for accurate determination of substrate concentration dependences, and misleading rate laws may be derived if this condition is not met.[3b] The example of Figure 3a and Scheme 4a illustrated a case where these assumptions clearly are not met, with a portion of the catalyst existing off the cycle in a reservoir whose concentration changes with reaction progress. While scenarios for off-cycle species have been proposed in a variety of reactions, the use of kinetic profiling to elucidate these cases has not yet become standard practice. Efforts to understand catalyst robustness in order to increase catalyst efficiency often rely on ex situ experiments, such as spectroscopic or crystallographic identification of inactive

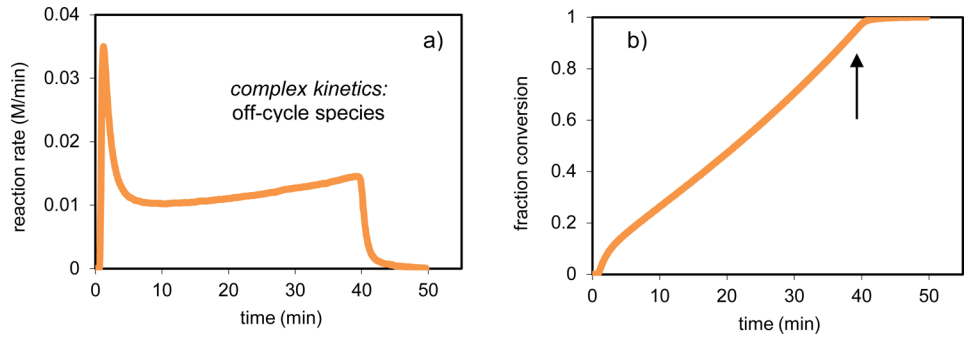

Figure 3. Kinetic profile of the organocatalyzed reaction shown in Scheme 3 under conditions given in Table 2, entry 4, (substrates **5c** and **6d**, catalyst **7d**). (a) Rate vs time; and (b) conversion vs time.

DOI: 10.1021/jacs.5b05841
J. Am. Chem. Soc. 2015, 137, 10852−10866

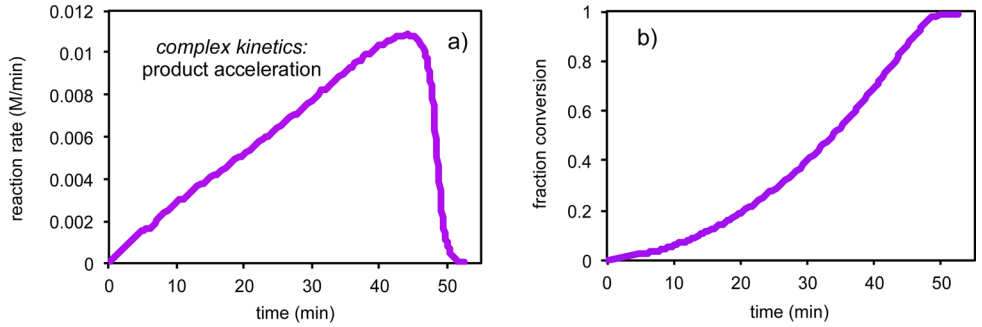

Figure 4. Kinetic profile of the organocatalyzed reaction shown in Scheme 3 under conditions given in Table 2, entry 5, (substrates **5c** and **6e**, catalyst **7b**. (a) Rate vs time; and (b) fraction conversion vs time.

Scheme 4. Added Complexity in the General Catalytic Cycle of Scheme 1 (See Figures 3 and 4)

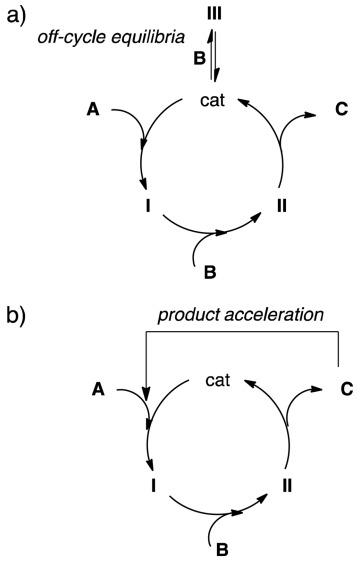

catalyst species, but it is not always easy to correlate such information with the working catalyst.

Ideally, a method that probes the active catalyst concentration under reaction conditions is best for assessing catalyst robustness, and the RPKA methodology known as the "same excess, [**xs**]" protocol was developed to address this concern. The protocol is illustrated in Table 3 for the Pd-catalyzed C–H

Table 3. Conditions of "Same [xs]" Reactions of Scheme 5 and Figure 5[a]

entry	[**8**] (M)	[**9**] (M)	[**10**] (M)	[**xs**]
1	0.22	0.26	0	0.05
2	0.11	0.17	0	0.05
3	0.11	0.17	0.11	0.05

[a]Ref 15b.

functionalization reaction shown in Scheme 5.[15] The reaction of Scheme 5 was monitored using ReactIR spectroscopy under the conditions shown in Table 3. Kinetic profiles of the concentration of substrate **8** vs time are shown in Figure 5.[15b]

The three reactions in Table 3 are carried out with the "same [**xs**]". The significance of this is that these conditions represent the same reaction started from different points: the initial substrate concentrations [**8**] and [**9**] for the reaction in entry 1 will equal those of the reaction in entry 2 when the former

Scheme 5. Pd-Catalyzed C–H Olefination of Arylacetic Acids[15]

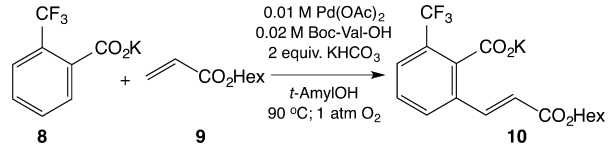

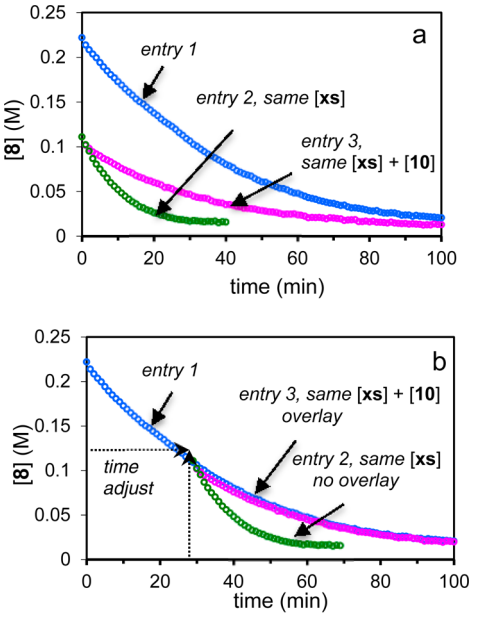

Figure 5. Kinetic profile of the reaction of Scheme 6.[14b] (a) same [**xs**]: blue (Table 3, entry 1); green (Table 3, entry 2); magenta: same [**xs**] + product [**10**] (Table 3, entry 3); (b) time-adjusted profiles for green and magenta reactions from part (a).

reaches 50% conversion. From that conversion onward, these two reactions exhibit the same temporal substrate concentrations; therefore, their kinetic profiles in Figure 5 should be identical from this point onward.

At the point in the reaction where the two profiles of entries 1 and 2 in Table 3 should begin to exhibit identical behavior, two possible differences exist between these two reactions that might help to rationalize cases where it is found that their behavior differs: (1) the reaction in entry 1 has undergone a number of catalyst turnovers, while the catalyst in entry 2 is fresh; and (2) the reaction vial for entry 1 contains 0.11 M product **10** while the reaction for entry 2 has not yet formed product. Thus, the kinetic profiles for the reactions of entry 1

DOI: 10.1021/jacs.5b05841
J. Am. Chem. Soc. 2015, 137, 10852–10866

and entry 2 of Table 3 provide a diagnostic for either catalyst deactivation or product inhibition.

The experiment in entry 3, Table 3, provides the means to distinguish between these two possibilities. In this case, product **10** has been added to a reaction with the same initial conditions as the reaction in entry 2. Thus, entry 3 describes a reaction where initial concentrations of not only substrates **8** and **9** but also product **10** are identical to those of the reaction in entry 1 at 50% conversion. If the kinetic profile of this reaction is identical to that of entry 2, catalyst deactivation is implicated; if it is identical to that of entry 1, product inhibition is implicated.

In order to compare the profiles the three reactions of Table 3 shown in Figure 5a, we create "time-adjusted" profiles simply by shifting the curves of entries 2 and 3 in time, as indicated by the arrows shown in Figure 5b, to the point where their concentrations are equal to that of the reaction of entry 1. Figure 5b shows a clear lack of overlay for entry 2 (same [**xs**]) and perfect overlay for entry 3 (same [**xs**] with product added), confirming that the origin of the sluggish rate over time is product inhibition.

Scheme 6 illustrates the case shown in Figure 5 in the lexicon of Scheme 1. When the reaction product interacts with one of

Scheme 6. Catalytic Cycle with Product Inhibition

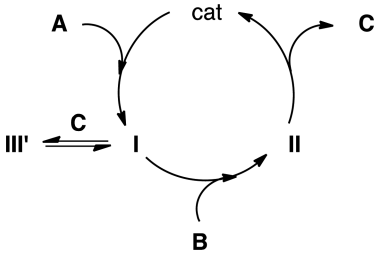

the catalytic intermediates off-cycle in a nonproductive manner, reaction rate will decrease with increasing reaction progress as the off-cycle equilibrium siphons more and more of the catalyst out of the active cycle. It is interesting to compare this case of product–catalyst interaction, which results in a rate slower than expected, as catalyst is pulled away from the main cycle, with that of substrate–catalyst interaction illustrated in Figure 4a and Scheme 4a, which results in a temporally rising rate as catalyst is pulled back into the cycle as the reaction progresses.

Take-Home Message. The same excess protocol provides a rapid means of elucidating whether the catalyst maintains its initial activity over many turnovers. In addition, a combination of three experiments can distinguish between product inhibition and other forms of catalyst deactivation. Simple manipulation of concentration profiles to probe for overlay in time-adjusted plots makes the same excess protocol straightforward to carry out even without converting reaction progress measurements from concentration to reaction rate. Understanding catalyst robustness is critical to developing an accurate kinetic analysis of a catalytic network.

Theme 5: Mechanistic Insights from Order in Catalyst Concentration. The same [**xs**] protocol allows us to assess the stability of the catalyst over time for reaction networks such as Scheme 1 or the variations presented in Schemes 4 and 6. One point to note is that all of these networks assume that the reaction is first order in [catalyst], and indeed most catalytic reactions obey first-order dependence in catalyst concentration. Exceptions include cases where dimer or higher order species may be formed on or off the catalytic cycle; palladacycle catalysts such as **3b** present one example,[4] and systems exhibiting nonlinear effects in catalyst enantiopurity, such as the diamino alcohol catalyzed dialkylzinc alkylation of aldehydes studied by Noyori,[16] represent another. In these cases a diagnostic for the presence of off-cycle dimeric species is the observation of an order in [catalyst] that is <1. The opposite case, an order in [catalyst] >1, is even more rare and indicates that two catalyst molecules must participate in a kinetically meaningful step in the cycle. Such an unusual case cannot be easily analyzed using standard mathematical treatments such as the King–Altman formalism[17] developed for enzyme-catalyzed reactions. Confirming the catalyst concentration dependence should be carried out routinely as a simple control experiment to rule out unusual cases or as a diagnostic to probe complex ones.

One striking example of second-order kinetics in [catalyst] is the hydrolytic epoxide ring-opening by Co(salen) catalysts discovered by Jacobsen (Scheme 7).[18] The order in [Co(salen]

Scheme 7. Hydrolytic Epoxide Ring Opening[18,19]

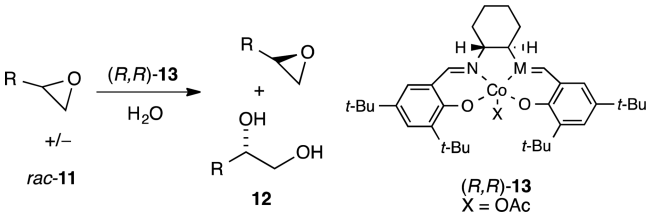

is confirmed by the overlay between two reactions carried out with enantiopure **11** at different catalyst **13** concentrations, with reaction progress data plotted as reaction rate/[cat]^2 vs [substrate], as shown in the inset in Figure 6.[19] A cooperative

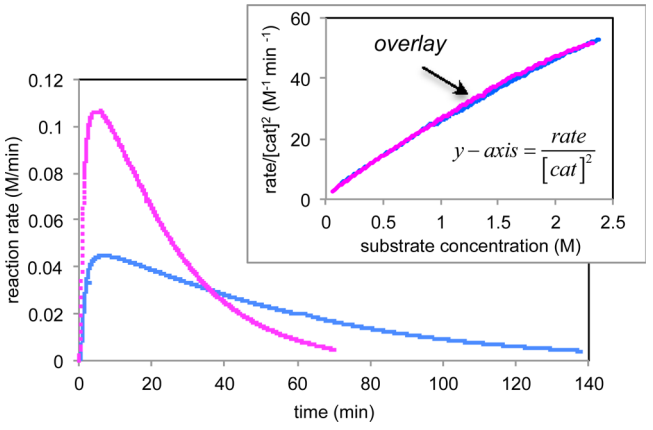

Figure 6. Reaction calorimetric rate profiles for the reaction in Scheme 7 carried out with 3.9 M **11** (R = 1-hexene), 2.9 M H_2O, 6.2 M butanediol additive, and 0.045 M **13** (magenta) or 0.028 M **13** (blue). Inset: data replotted as rate/[**13**]^2 vs [H_2O].

bimolecular reaction between two catalyst molecules, with one bound to the electrophilic epoxide substrate **A** and the other bound to the nucleophile **B** (water in this case), constitutes the turnover-limiting step. This system may be described by a modification to the simple network of Scheme 1 as given in Scheme 8, where two catalytic cycles cooperate to produce product **C** from the bimolecular reaction between catalytic intermediates **I** and **I′** (epoxide and nucleophile-bound Co(salen), respectively).

DOI: 10.1021/jacs.5b05841
J. Am. Chem. Soc. 2015, 137, 10852–10866

Scheme 8. Second-Order Dependence on Catalyst via Cooperative Bimolecular Reaction

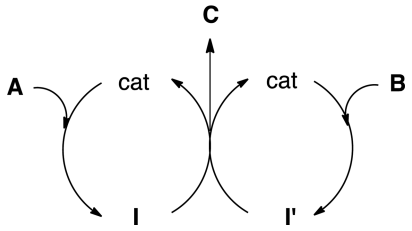

Take-Home Message. While most catalytic reactions exhibit first-order kinetics in [catalyst], observation of nonfirst-order kinetics is diagnostic for unusual mechanistic behavior, including the formation of dimeric or higher order off-cycle species (giving orders lower than one) as well as bimolecular reaction between two catalyst species (giving orders higher than one).

Theme 6: Mechanistic Clues from Competitive Reactions. Competitive reactions may be employed in a diagnostic fashion to probe reaction mechanisms, with examples including Hammett correlations and kinetic isotope effects. Because two parallel pathways compete for the same pool of catalyst species, the intrinsic reactivity or stability of kinetically important species on one pathway may influence the outcome of the reaction on the other pathway and in some cases in ways that might not be expected by consideration of each pathway separately. We return to the Pd(binap)-catalyzed amination of aryl halides (Scheme 2) for an illustration of general mechanistic implications for parallel reaction networks.[20] Figure 7a shows the kinetic profiles for the separate reactions of aryl halide **1c** with either 1-hexylamine **2a** or benzophenone hydrazone **2c**. Overall first-order kinetics are observed in the reaction of **2a**, similar to the reaction of Figure 1a; however, overall zero-order kinetics and a much slower overall rate are observed with **2c** as the amine substrate.

Following the discussion in Theme 2, the difference in these rate profiles may be rationalized by considering that the turnover-limiting step of the reaction shifts from oxidative addition (addition of **A** to **cat** in the lexicon of Scheme 1) for the reaction of **2a**, to reductive elimination (reaction of intermediate **III**) for the reaction of **2c**. Because the reaction of **2c** is significantly slower than that of **2a**, it might be considered reasonable to predict that, in competitive reactions where the two substrates are present in the same flask, **2a** would react preferentially. Strikingly, however, as shown in Figure 7b, the inverse result was observed: The lower reactivity, zero-order reaction of **2c** preceded the faster, first-order reaction of **2a**. Substrate **2a** did not begin to react until **2c** was converted completely to product.

Scheme 9 shows the basic network of Scheme 1 expanded to describe this case, the competition between two substrates **B** and **B′** for intermediate **I** formed by reaction of **cat** with substrate **A**. Applied to the reactions shown in Figure 7, the scheme highlights that for substrate **A** = **1c** and **B** = **2a**, the addition of **A** to **cat** is turnover-limiting, and **cat** is the resting state. When **B′** = **2c**, **II′** is the resting state, and its reaction is turnover-limiting.

While the 1-hexylamine **B** pathway (to form **C**) is intrinsically much faster than the benzophenone hydrazone **B′** pathway to form **C′**, the different results observed in the competitive reaction, where the two networks share the same

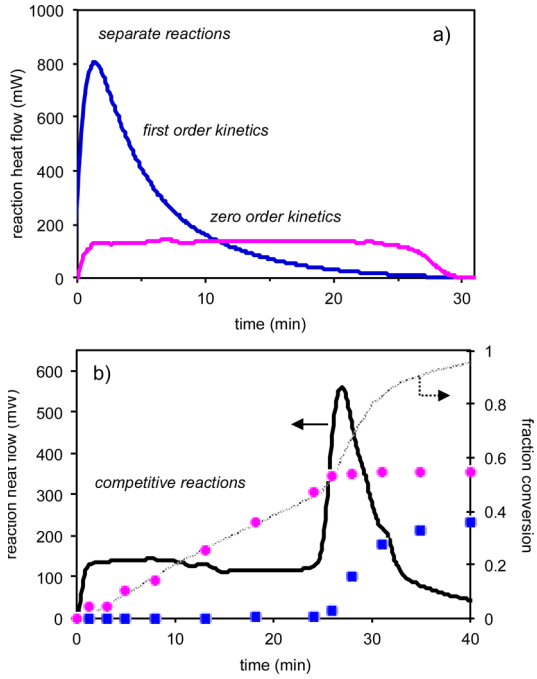

Figure 7. (a) Reaction calorimetric rate profiles for separate reactions of **2a** and **2c** with **1c** (see Scheme 2). Conditions: 0.3 M **1c**; 0.4 M; **2a** (blue line) or **2c** (magenta line); 0.45 M Na^{t}BuOOH in toluene using 3 mol % **3a**. Reaction of **2a** at 70 °C; reaction of **2c** at 90 °C. (b) Reaction calorimetric rate profiles for competitive reactions of **2a** and **2c** with **1c** at 90 °C (see Scheme 2). Conditions: **1c**; 0.47 M; 0.25 M each **2a** and **2c**; 0.55 M Na^{t}BuOOH in toluene using 1.9 mol % **3a**. Solid black line: heat flow in mW; gray line: fraction conversion derived from integration of the heat flow curve. Symbols represent fraction conversion of **1c** to **4a** (open squares) and to **4c** (open circles) measured by GC.

Scheme 9. Competitive Reactions with Differing Resting States (See Figure 5)

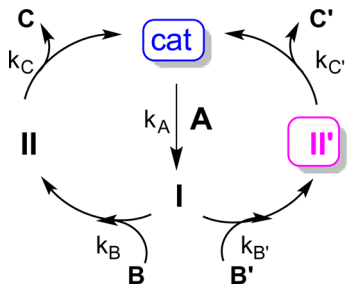

catalyst pool, suggest two possible explanations. If the addition of **B** and **B′** to **I** is irreversible, then the competitive experiment tells us that $k_{B'} \gg k_B$. This information is not available from the kinetic data of either reaction carried out separately, because this step precedes the turnover-limiting step in the case of **B** and is subsequent to the turnover-limiting step in the case of **B′**. If, on the other hand, the addition of **B** and **B′** to **I** is reversible, then the rate profiles under competitive conditions tell us that species **II′** is significantly more stable than any other species in the network, meaning that the catalyst rests virtually completely at **II′** until all of the **B′** has reacted. This behavior has been suggested in the present case, referred to as "monopolizing kinetics"[20] since **II′** monopolizes the catalyst to the exclusion of the **B** cycle. In either the irreversible or the reversible scenario, the competitive reaction allows us to obtain

DOI: 10.1021/jacs.5b05841
J. Am. Chem. Soc. 2015, 137, 10852−10866

information about elementary steps that are kinetically invisible in the separate cycles.

A further example of a competitive reaction is shown in Scheme 10.[21,22] Hydrogenation of allylic alcohols using

Scheme 10. Asymmetric Hydrogenation Catalyzed by Ru(*S*)-binap[22]

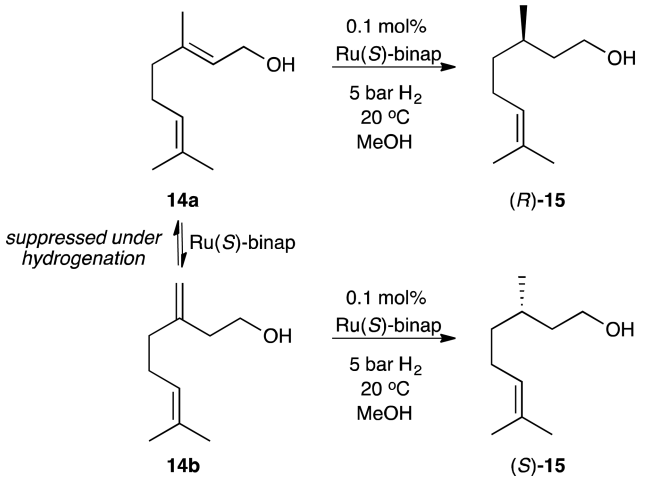

Ru(binap) catalysts is an early classic example of asymmetric catalysis introduced by Noyori and co-workers.[21] Our own kinetic investigations of the reaction of **14a** led to the unusual profile shown in Figure 8. A rapid rate was observed in the

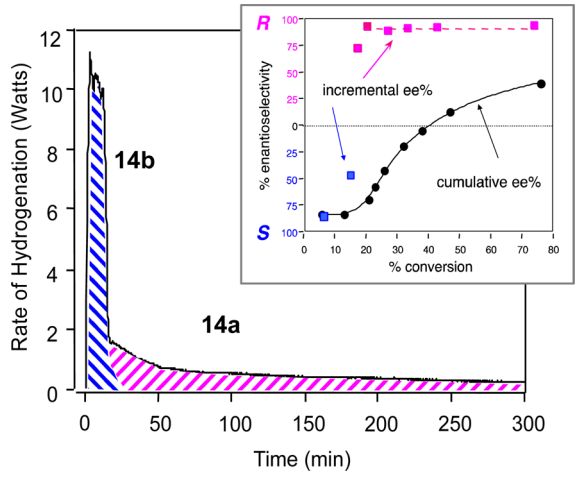

Figure 8. Reaction calorimetric rate profile for the hydrogenation reaction of Scheme 10 using Ru-(*S*)-binap). Hashed blue line represents the rapid initial reaction of **14b** (formed by isomerization of **14a** prior to reaction) to ca. 15% conversion; hashed magenta lines represent the latter 80% conversion of **14a** that proceeds more slowly and continues for several hours longer than shown here. Inset: evolution of the ee of reaction product **15** as a function of conversion. Incremental ee is calculated as the ee of the reaction product formed between two conversion points.

beginning of the reaction, dropping dramatically by an order of magnitude after ca. 15% conversion. This unusual reactivity was accompanied by an enantiomeric excess (ee) profile that shifted from unexpectedly high ee to (*S*)-**15** toward (*R*)-**15**, the expected reaction product.

This puzzling behavior was rationalized by the discovery that Ru(*S*)-binap catalyzes an isomerization pathway between geraniol **14a** and the terminal homoallylic alcohol γ-geraniol **14b**. Separate reactions of the two revealed that while **14a** gives high ee to (*R*)-**15**, the reaction of **14b** produces (*S*)-**15** in equally high ee and at a much faster rate. Extended contact between **14a** and the catalyst prior to introduction of hydrogen produces a mixture of ca. 85% **14a** and 15% **14b**, which react to form (*R*)-**15** and (*S*)-**15**, respectively, after introduction of hydrogen. The much higher reactivity of the terminal olefin **14b** resulted in its complete conversion (hashed blue area in Figure 7) before **14a** had undergone significant conversion. Calculation of the incremental ee value for each fraction of the conversion showed that the trend was not a gradual shift but a step change corresponding to the drastic change from reaction of **14b** to that of **14a**.

The general case of such a competitive network is shown in Scheme 11. When products **C** and **C′** are enantiomers, the final

Scheme 11. Competitive Catalytic Cycles of an Interconverting Substrate That Forms Different Products

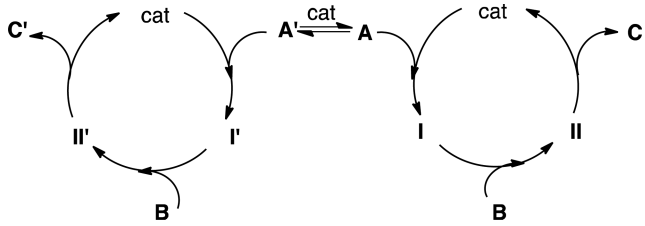

ee value resulting from the reaction under conditions where both **A** and **A′** are present will not be representative of the selectivity of the catalyst for either substrate. For the case of the reaction of Scheme 10, the rapid reaction of **14b** made its identification during by NMR elusive, and without the clues provided by the kinetic profile and the temporal ee measurement, the isomerization pathway might not have been uncovered.

Take-Home Message. Two examples demonstrate how monitoring competitive reactions may provide mechanistic clues to multistep catalytic reactions. The competitive network may make it possible to learn about the reactivity and stability of intermediates that may not be observable by studying each single reaction cycle. Kinetic profiling of the reaction time course can be diagnostic for behavior that might be hidden by examination of final product selectivity alone. In addition, these results indicate that care must be taken in mechanistic interpretation of the results of competitive reactions because the observations may not be in accord with those from the reactions studied separately.

Theme 7: Multiple Orthogonal Methods for Kinetic Profiling. One key prerequisite for reaction progress kinetic analysis using in situ monitoring tools is the assurance that the reaction progress measuring technique employed in fact monitors the reaction of interest. Validation of the method may be established by comparing the results to those of another known method; typically in situ FTIR spectroscopy or reaction calorimetric curves are compared to a known compositional analysis method by HPLC or GC. Comparing two different methods that use different properties to measure reaction progress not only validates the method but may also contribute to the mechanistic insight offered by in situ analysis. Two examples given below illustrate this point.

The autocatalytic Soai reaction[23−25] shown in Scheme 12 provides a rare example of a reaction that is catalyzed by its own

DOI: 10.1021/jacs.5b05841
J. Am. Chem. Soc. 2015, 137, 10852−10866

Scheme 12. Soai Autocatalytic Reaction with Amplification of Enantiomeric Excess.[24]

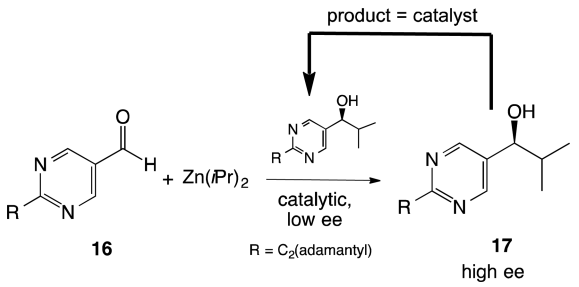

reaction product. The reaction exhibits amplification of enantiomeric excess, with the ee increasing as reaction turnover increases. This reaction provides the first experimental example of theoretical models for understanding the emergence of biological homochirality.[26] The reaction also offers challenges for classical kinetic analysis; initial rate measurements may not provide useful information in a reaction where the amount of catalyst and product selectivity both change with each catalytic turnover!

Reaction calorimetric monitoring provided the temporal rate curve shown in Figure 9a.[24] The kinetic profile exhibits a constant, low (but nonzero) heat flow during this induction period. One might be tempted to suggest that reaction turnover was not occurring during this time and that the apparent nonzero heat flow is simply due to a baseline shift. Converting the heat flow curve to temporal conversion according to eq 1b and comparing the same reaction monitored by ReactIR spectroscopy, which monitors substrate concentration directly according to eq 3a, provide the plots in Figure 9b. The low reaction heat flow matches the direct measurement of substrate conversion during the induction period.

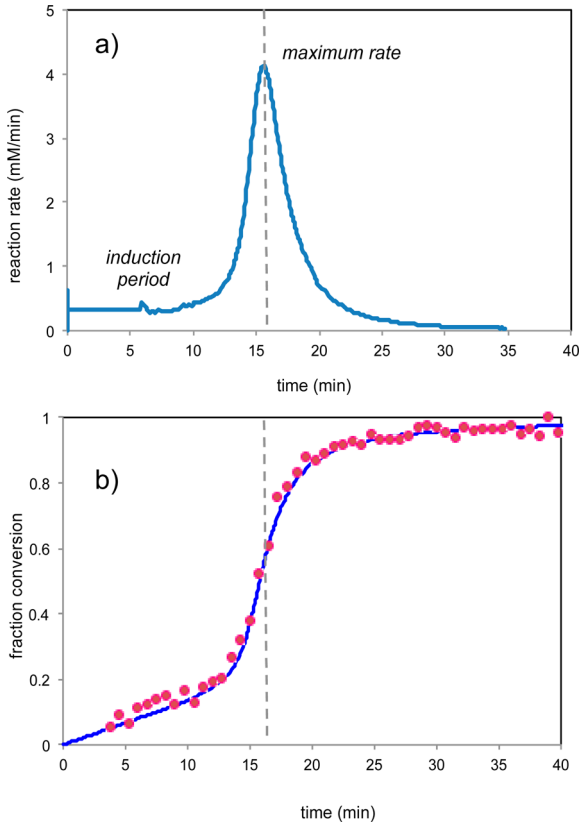

Figure 9. Kinetic profiles of the Soai reaction of Scheme 12 with 24 mM **16**, 48 mM Zn(*i*Pr)$_2$, 0.52 mol % **17** as catalyst, toluene °0 C. (a) Reaction calorimetric rate profile; and (b) conversion vs time from integration of the heat flow curve of part (a) (solid line) and from concentration vs time measurements from in situ ReactIR spectroscopy (red symbols).[24b]

The mechanistic interpretation of the initial slow reaction is that it represents the noncatalyzed formation of **17** and is thought to lead to self-assembly of the active autocatalytic species, which is suggested to be a dimeric or tetrameric species.[25] Observation of an extended induction period is in accordance this mechanism, summarized in Scheme 13, again in the lexicon of Scheme 1. The combination of the two kinetic profiling tools confirms the significance of this induction period and shows that it cannot be neglected in kinetic analysis.

Scheme 13. Autocatalytic Reaction Network Coupled to the Initial Non-Catalyzed Product-Forming Reaction

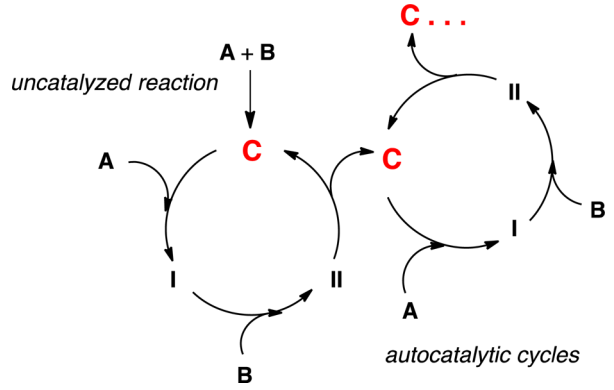

Figure 9 also underscores how we may compare the same features of the reaction in the temporal conversion curve and the reaction rate curve. The rate maximum, which is the most prominent feature of the rate vs time curve, appears as an almost indiscernable inflection point when the data are plotted as conversion vs time. This highlights one of the advantages of reaction calorimetry, which yields rate as the primary data. Concentration data may be converted to rate by taking the derivative, but this process inevitably introduces a level of noise in the data that it not observed with rate as a direct measurement.

The combination of complementary techniques to measure conversion as in Figure 9 is important in a more general way for any kinetic investigation employing an in situ tool. It is imperative to confirm that the kinetic profile obtained is indeed a reflection of the kinetics of the reaction under study. This is typically done by comparing a new in situ method to an established and accepted method such as chromatographic analysis or NMR spectroscopy.

A final example to highlight the power of multiple kinetic profiling tools in extracting mechanistic information is presented in Scheme 14.[27] Chiral piperazine **20** is formed from pyrazine **18** via consecutive hydrogenation steps. This reaction network differs from the systems so far under discussion in that intermediate **19** is the product of one catalytic cycle, which then re-engages the catalyst in a second cycle to form the final product **20**. This is depicted in Scheme 13 modified from the general case of Scheme 1 to include two

DOI: 10.1021/jacs.5b05841
J. Am. Chem. Soc. 2015, 137, 10852−10866

cycles, where the reaction product of the first becomes the substrate of the second.

The desired (*S*)-piperazine-2-^{t}Bu-carboxamide is an intermediate in the synthesis of Merck's anti-HIV protease inhibitor, Crixivan. Two potential intermediates **19** are possible, from addition of either one molecule of hydrogen (**19a**, dihydro intermediate) or two molecules of hydrogen (**19b**, tetrahydro intermediate), with the most stable structures for each predicted by molecular modeling.[27a] While the reaction catalyzed by heterogeneous Pd/C forms racemic product, an enantioselective catalytic process for the final hydrogenation step might be developed if the prochiral tetrahydro intermediate **19b** could be isolated.[28]

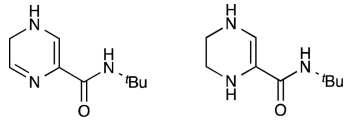

19a **19b**

The reaction of Scheme 14 was monitored simultaneously by *three* different in situ tools: reaction calorimetry, ReactIR

Scheme 14. Sequential Hydrogenation Reaction in the Synthesis of Crixivan[27]

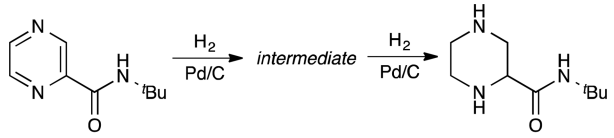

18 **19** **20**

spectroscopy, and H_2 pressure uptake. FTIR spectroscopy was able to detect only one intermediate species,[26b] as shown in Figure 10. Kinetic modeling of the sequential hydrogenation at

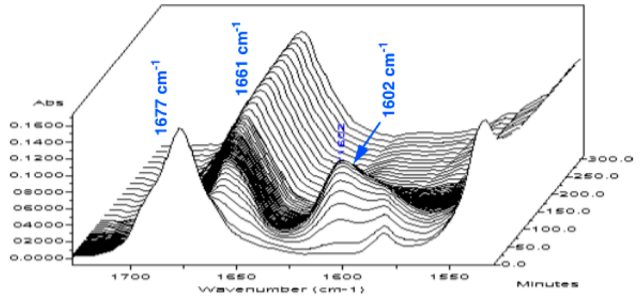

Figure 10. Reaction of Scheme 14 monitored by ReactIR spectroscopy at 60 °C under 1 atm H_2 in ^{i}PrOH;[26b] [**15**] = 0.5 M; 5 wt % Pd/C. Substrate **18** at 1677 cm^{-1}, product **20** at 1661 cm^{-1}, and the unknown intermediate **19** at 1602 cm^{-1}.[27b]

different temperatures was carried out[27a] to determine conditions under which the concentration of **19** could be maximized. Kinetic profiles of the reaction of Scheme 14 shown in Figure 11 reveal that at low temperature, high concentrations of **19** were obtained at near complete consumption of **18** and before significant production of **20** (dashed vertical line in Figure 11), suggesting that at 35 °C completion of the first cycle in Scheme 15 occurs before the second cycle gets underway. Identification of intermediate **19**—the dihydro or tetrahydro species—may be addressed by the use of multiple in situ tools. The compositional information offered by the ReactIR was combined with hydrogen uptake and heat flow

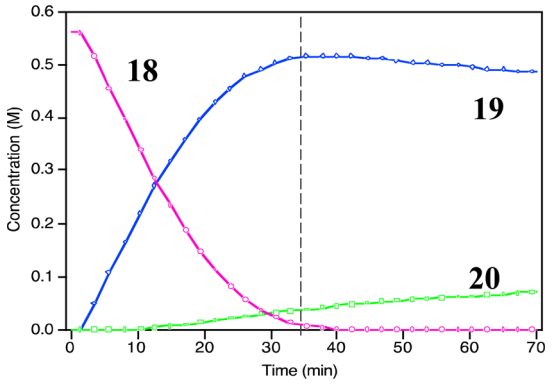

Figure 11. Kinetic profile of the reaction of Scheme 14 at 35 °C monitored by ReactIR spectroscopy.[27b] Dashed line shows maximum concentration of **19** formed when **18** is consumed and before significant **20** is formed.

Scheme 15. Sequential Catalytic Cycles

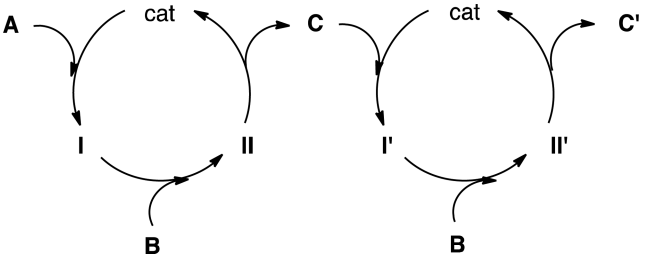

data, assessed at the point of maximum concentration of intermediate **19** (dashed line in Figure 11).

As shown in Table 4, the combination of three different in situ tools that measure different physical and chemical

Table 4. Theoretical and Experimental Data for Identification of Intermediate 19[27]

technique	dihydro (calculated)	tetrahydro (calculated)	**19** (experimental)
H_2 uptake	10 kcal/mol H_2	14 kcal/mol H_2	13.3 kcal/mol H_2
calorimetry	9.9 kcal/mol **18**	27.7 kcal/mol **18**	26 kcal/mol **18**

properties of the reacting system enabled a definitive identification of the intermediate as **19b**, the tetrahydro species. Comparison of reaction heat flow and the H_2 uptake at the time of the dashed line in Figure 11, with maximum buildup of **19** prior to significant production of product **20**, allows calculation of the heat evolved per substrate molecule **18** reacted and heat evolved per H_2 molecule consumed. These experimental values given in the last column of Table 4 may be compared with predicted heats of formation of the dihydro and tetrahydro intermediates calculated using a semiempirical quantum mechanical model.[27a] It is clear that the experimental data correspond closely to the values predicted for species **19b** to be the desired tetrahydro intermediate.

Take-Home Message. Two examples illustrate the advantages of employing multiple in situ tools for monitoring reaction progress. First, finding agreement between two different methods of measuring reaction progress helps to validate both techniques and provides confidence that the tools are indeed monitoring the progress of the desired reaction. Second, tools that correlate with reaction progress by measuring different physical and chemical properties can be

DOI: 10.1021/jacs.5b05841
J. Am. Chem. Soc. 2015, 137, 10852−10866

combined to provide increased mechanistic insight and may help distinguish conclusively between different proposed intermediates.

RECOMMENDATIONS

The use of RPKA has become widespread in pharmaceutical process chemistry groups[29] where the advantage of obtaining accurate kinetic information in a rapid and systematic fashion with fewer experiments aligns with the FDA's "Quality by Design (QbD)" paradigm for the production of pharmaceuticals.[30] Software designed to carry out the manipulations to produce "graphical rate equations" is available, along with webinars that explain the theory and procedures.[31] A Wikipedia page has been written (not by the author of this paper!) that describes the methodology.[32] More recently, publications utilizing the methodology have begun to appear in the literature from academic synthetic chemistry laboratories carrying out mechanistic investigations.[33]

Based on our extensive experience with a variety of different reactions, our laboratories have developed a simple and general protocol for initiating a kinetic analysis of any new reaction. Typically we begin after an initial screening of parameters such as solvent, catalyst, additives, temperature, which allows us to establish a range of conditions where the reaction appears to be well-behaved. Here we outline this protocol for a reaction of the type of **A** + **B** → **C**.

Step 1 designates a set of reaction conditions, most specifically, initial substrate and catalyst concentrations, along with temperature, pressure, solvent, and additives, that we term "standard conditions." All further experiments will be referred to these conditions. At this stage, it may also be useful to define a range of concentrations, and relative concentrations, of reactants **A** and **B** under which the reaction might reasonably be carried out. Temperature, pressure, solvent, and additives are kept constant over the series of experiments described here.

Step 2 defines a further set of conditions for the "same excess" protocol by changing the initial concentrations of *both* substrates **A** and **B**, keeping their *difference* ($[\mathbf{B}]_0 - [\mathbf{A}]_0$) constant, as was shown in eq 4. The amount by which the standard condition concentrations are changed to provide same excess experimental conditions will depend on the reaction under study. The development of a practical range of concentrations from Step 1 aids in choosing reasonable "same excess" conditions. Note that the absolute concentration of catalyst (not the mol%!) is held constant between the standard, same excess, and different excess conditions.

Our practice is to complete the standard and "same excess" experiments first, since it is important to establish from the beginning whether lack of catalyst robustness will be problematic in understanding the reaction mechanism. Once the results from the "same excess" protocol have established the presence or absence of complicating factors such as catalyst deactivation or product inhibition, we move on to determine the substrate concentration dependences. It should be noted that observed orders in substrate concentrations [**A**] and [**B**] may be altered from those predicted from fundamental mechanistic proposals in cases where these complicating factors have a significant influence on rate. A nonrobust system does not preclude further mechanistic analysis, but it may limit the range of reaction progress data that will be useful in probing for reaction orders, turnover-limiting steps, and catalyst resting state. For example, "same excess" experiments may tell us that catalyst deactivation is more significant toward the end of the reaction, in which case we might use only the first 50% conversion in our kinetic analysis.

Step 3 defines at least one further set of conditions of "different excess". Any concentrations may be chosen for $[\mathbf{A}]_0$ and $[\mathbf{B}]_0$, within the reasonable range defined in Step 1, as long as their difference ($[\mathbf{B}]_0 - [\mathbf{A}]_0$) is not the same as in the standard conditions. Typically we choose two further "different excess" experiments by taking the conditions defined in either Steps 1 or 2 and changing one or the other of the starting concentrations, $[\mathbf{A}]_0$ or $[\mathbf{B}]_0$, in turn, while leaving the other the same. This makes a direct qualitative comparison of kinetic profiles straightforward in cases where concentration/time data are employed directly, without first converting to rate/time data. It is important to note that all of the analysis presented in this work may be carried out using experimental methodology that measures concentration rather than rate directly.

Figure 12 illustrates this point for the reaction that was presented in Scheme 5. In addition to the results for standard conditions, plots for two "different excess" experiments are shown, where the initial concentration of each of the substrates in turn has been altered from standard conditions while leaving the other substrate's initial concentration identical to the standard conditions. This experimental design allows at least qualitative—and often quantitative—determination two of substrate concentration dependences from just three separate experiments.[15b] In this example, we find that the reaction exhibits zero-order dependence on [**8**] (identical rates observed for different [**8**]) and a negative-order dependence on [**9**] (slower conversion observed for higher [**9**]).

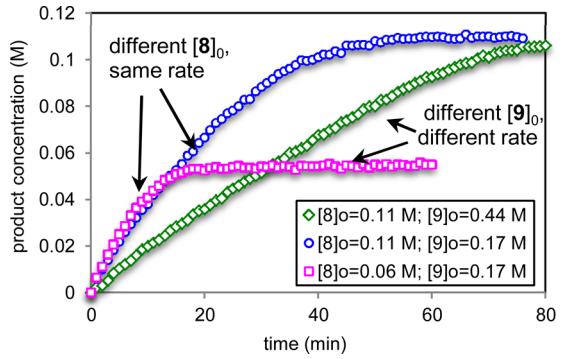

Figure 12. Illustration of experiments from Step 1 (standard) and Step 3 (different excess) of the protocol outlined for initial kinetic analysis using RPKA, using the reaction of Scheme 5. Blue circles: standard conditions (entry 2 of Table 3); Green diamonds: same $[\mathbf{8}]_0$ as standard, changing $[\mathbf{9}]_0$; and magenta squares: same $[\mathbf{9}]_0$ as standard, changing $[\mathbf{8}]_0$. These three experiments coupled with Step 2 (same excess) experiment (Table 3, entry 1) provide the initial kinetic analysis of the reaction.

This three-step protocol encompassing four experiments, standard conditions, "same excess," and two "different excess" experiments, provides a comprehensive, if in some cases preliminary, kinetic analysis of any new reaction. In the best case scenario, this straightforward protocol confirms that the catalyst is robust and provides reaction orders in [**A**] and [**B**]. In more complicated cases, these experiments serve as a preliminary analysis alerting us that the reaction under study exhibits complexity beyond the simple reaction network of Scheme 1 and that more work needs to be done. It is in these more complicated cases that we often look to the qualitative form of the kinetic profiles to provide clues to further

DOI: 10.1021/jacs.5b05841
J. Am. Chem. Soc. 2015, 137, 10852−10866

experiments that will help unravel those complexities, as we have shown for many of the examples in this Perspective.

CONCLUSIONS

The seven themes and seven "take-home messages" discussed in this Perspective begin to reveal the rich mechanistic information that may be extracted from kinetic profiles of catalytic reaction networks. The profile can infer the turnover-limiting step and catalyst resting state; examples of the resting state as each of the species **cat**, **I**, or **II** in the simple cycle of Scheme 1 are illustrated. The importance of elucidating not only substrate concentration dependences but also the order in [catalyst] and the robustness of the catalytic cycle is emphasized. Kinetic profiles are shown to be invaluable diagnostic tools as layers of complexity are added to the simple cycle of Scheme 1, including off-cycle equilibria, product feedback loops, and competitive reactions. The combination of multiple in situ techniques may help to solve mechanistic puzzles by providing information about different aspects of complex reaction networks. In summary, the kinetic profile provides a window inside the catalytic network, chronicling its story from beginning to end. The step-by-step protocol outlined here enables an initial kinetic analysis, providing information that can be used to suggest further experiments using other tools to add to the mechanistic detail sketched in by the kinetics. These examples demonstrate that carrying out kinetic analysis at the outset of a reaction investigation can tell us where to look for clues that may be key to unlocking the reaction mechanism for both simple and complex catalytic reactions.

AUTHOR INFORMATION

Corresponding Author

*blackmond@scripps.edu

Notes

The authors declare no competing financial interest.

ACKNOWLEDGMENTS

The author is grateful for many stimulating interactions with co-workers and collaborators over the past 20 years whose work is discussed in this review and who are cited in the references below. I would like to acknowledge in particular collaborations with Y.-K. Sun, J. R. Sowa, Jr., A. Pfaltz, J. M. Brown, S. L. Buchwald, E. N. Jacobsen, A. Armstrong, and J.-Q. Yu.

REFERENCES

(1) Attribution goes to an anonymous reviewer for the "straight line" comment; I am indebted to Dave Collum for the "take-home message" concept I use in this review, which he uses to great advantage in his kinetics courses.

(2) (a) Blackmond, D. G. *Angew. Chem., Int. Ed.* **2005**, *44*, 4302. (b) Mathew, J. S.; Klussmann, M.; Iwamura, H.; Valera, F.; Futran, A.; Emanuelsson, E. A. C.; Blackmond, D. G. *J. Org. Chem.* **2006**, *71*, 4711. (c) Zotova, N., Iwamura, H., Mathew, S. P. Blackmond, D. G. In *Trends in Process Chemistry*; Braish, T., Gadasamatti, K., Eds.; CRC Press: New York, 2008; p 455.

(3) (a) Shekhar, S.; Ryberg, P.; Hartwig, J. F.; Mathew, J. S.; Blackmond, D. G.; Strieter, E. R.; Buchwald, S. L. *J. Am. Chem. Soc.* **2006**, *128*, 3584. (b) Blackmond, D. G.; Schultz, T.; Mathew, J. S.; Loew, C.; Rosner, T.; Pfaltz, A. *Synlett* **2006**, *18*, 3135.

(4) Rosner, T.; Le Bars, J.; Pfaltz, A.; Blackmond, D. G. *J. Am. Chem. Soc.* **2001**, *123*, 1848.

(5) List, B.; Lerner, R. A.; Barbas, C. F., III. *J. Am. Chem. Soc.* **2000**, *122*, 2395.

(6) Ahrendt, K. A.; Borths, C. J.; MacMillan, D. W. C. *J. Am. Chem. Soc.* **2000**, *122*, 4243.

(7) MacMillan, D. W. C. *Nature* **2008**, *455*, 304.

(8) Brochu, M. P.; Brow, S. P.; MacMillan, D. W. C. *J. Am. Chem. Soc.* **2004**, *126*, 4108.

(9) (a) Burés, J.; Armstrong, A.; Blackmond, D. G. *J. Am. Chem. Soc.* **2012**, *134*, 14264. (b) Wiest, J., Masters' Thesis, University of Basel, 2012.

(10) (a) Zotova, N.; Broadbelt, L. J.; Armstrong, A.; Blackmond, D. G. *Bioorg. Med. Chem. Lett.* **2009**, *19*, 3934. (b) Zotova, N.; Franzke, A.; Armstrong, A.; Blackmond, D. G. *J. Am. Chem. Soc.* **2007**, *129*, 15100.

(11) Burès, J.; Armstrong, A.; Blackmond, D. G. *Angew. Chem., Int. Ed.* **2014**, *53*, 8700.

(12) (a) Tiecco, M.; Carlone, A.; Sternativo, S.; Marini, F.; Bartoli, G.; Melchiorre, P. *Angew. Chem., Int. Ed.* **2007**, *46*, 6882. (b) Sunden, H.; Rios, R.; Cordova, A. *Tetrahedron Lett.* **2007**, *48*, 7865.

(13) Hein, J. E.; Armstrong, A.; Blackmond, D. G. *Org. Lett.* **2011**, *13*, 4300.

(14) (a) Mathew, S. P.; Iwamura, H.; Blackmond, D. G. *Angew. Chem., Int. Ed.* **2004**, *43*, 3317. (b) Mathew, S. P.; Klussmann, M.; Iwamura, H.; Wells, D. H., Jr.; Armstrong, A.; Blackmond, D. G. *Chem. Commun.* **2006**, 4291. (c) Zotova, N.; Moran, A.; Armstrong, A.; Blackmond, D. G. *Adv. Synth. Catal.* **2009**, *351*, 2765.

(15) (a) Engle, K. M.; Wang, D.-H.; Yu, J.-Q. *J. Am. Chem. Soc.* **2010**, *132*, 14137. (b) Baxter, R. D.; Sale, D.; Engle, K. M.; Yu, J.-Q.; Blackmond, D. G. *J. Am. Chem. Soc.* **2012**, *134*, 4600.

(16) Kitamura, M.; Suga, S.; Oka, H.; Noyori, R. *J. Am. Chem. Soc.* **1998**, *120*, 9800.

(17) Cornish-Bowden, A. *Fundamentals of Enzyme Kinetics*, 2nd ed.; Protland Press: London, 1995; Chpt. 4.

(18) Tokunaga, M.; Larrow, J. F.; Kakiuchi, F.; Jacobsen, E. N. *Science* **1997**, *277*, 936.

(19) (a) Nielsen, L. P. C.; Stevenson, C. P.; Blackmond, D. G.; Jacobsen, E. N. *J. Am. Chem. Soc.* **2004**, *126*, 1360. (b) Luchi, J.; Blackmond, D. G.; Jacobsen, E. N.; unpublished data. (c) Nielsen, L. P. C.; Zuend, S. J.; Ford, D. D.; Jacobsen, E. N. *J. Org. Chem.* **2012**, *77*, 2486.

(20) (a) Ferretti, A. C.; Mathew, J. S.; Ashworth, I.; Purdy, M.; Brennan, C.; Blackmond, D. G. *Adv. Synth. Catal.* **2008**, *350*, 1007. (b) Ferretti, A. C.; Mathew, J. S.; Blackmond, D. G. *Ind. Eng. Chem. Res.* **2007**, *46*, 8584. (c) Ferretti, A.; Brennan, C.; Blackmond, D.G. *Inorg. Chim. Acta* **2011**, *369*, 292.

(21) (a) Takaya, H.; Ohta, T.; Inoue, S.-I.; Tokunaga, M.; Kitamura, M.; Noyori, R. *Org. Synth.* **1993**, *72*, 74. (b) Noyori, R.; Takaya, H. *Acc. Chem. Res.* **1990**, *23*, 345.

(22) (a) Sun, Y.; LeBlond, C.; Wang, J.; Blackmond, D. G.; Laquidara, J.; Sowa, J. R., Jr. *J. Am. Chem. Soc.* **1995**, *117*, 12647. (b) Sun, Y.; Wang, J.; LeBlond, C.; Reamer, R. A.; Laquidara, J.; Sowa, J. R.; Blackmond, D. G. *J. Organomet. Chem.* **1997**, *548*, 65. (c) Sun, Y.; Wang, J.; LeBlond, C.; Landau, R. N.; Laquidara, J.; Sowa, J. R.; Blackmond, D. G. *J. Mol. Catal. A: Chem.* **1997**, *115*, 495.

(23) Soai, K.; Shibata, T.; Morioka, H.; Choji, K. *Nature* **1995**, *378*, 767.

(24) (a) Gehring, T.; Quaranta, M.; Odell, B.; Blackmond, D. G.; Brown, J. M. *Angew. Chem., Int. Ed.* **2012**, *51*, 9539. (b) Hein, J. E.; Gherase, D.; Blackmond, D. G. *Top. Curr. Chem.* **2013**, *333*, 83.

(25) (a) Buono, F. G.; Blackmond, D. G. *J. Am. Chem. Soc.* **2003**, *125*, 8978−8979. (b) Quaranta, M.; Gehring, T.; Odell, B.; Brown, J. M.; Blackmond, D. G. *J. Am. Chem. Soc.* **2010**, *132*, 15104.

(26) (a) Frank, F. C. *Biochim. Biophys. Acta* **1953**, *11*, 459−463. (b) Calvin, M. *Molecular Evolution*; Oxford University Press, Oxford, 1969. (b) Blackmond, D. G. *Proc. Natl. Acad. Sci. U. S. A.* **2004**, *101*, 5732−5736.

(27) (a) Landau, R. N.; Singh, U. K.; Gortsema, F. P.; Sun, Y.; Gomolka, S. C.; Lam, T.; Futran, M.; Blackmond, D. G. *J. Catal.* **1995**, *157*, 201−208. (b) LeBlond, C.; Larsen, R.; Orella, C.; Forman, A.; Landau, R. N.; Laquidara, J.; Sowa, J. R.; Blackmond, D. G. *Thermochim. Acta* **1996**, *289*, 189.

DOI: 10.1021/jacs.5b05841
J. Am. Chem. Soc. 2015, 137, 10852−10866

(28) Pye, P. J.; Rossen, K.; Reamer, R. A.; Tsou, N. N.; Volante, R. P.; Reider, P. J. *J. Am. Chem. Soc.* **1997**, *119*, 6207.
(29) Kedia, S. B.; Mitchell, M. B. *Org. Process Res. Dev.* **2009**, *13*, 420.
(30) Yu, L. X. *Pharm. Res.* **2008**, *25*, 781.
(31) Mettler Autochem iC Kinetics software: http://us.mt.com/us/en/home/products/L1_AutochemProducts/AutoChem_software/iC-Kinetics.html; the software addresses the question of what constitutes a statistically accepatable "overlay" in graphical rate equations to determine reaction orders. A free on-demand webinar is also available from Mettler Autochem: http://www.pharmaceuticalonline.com/doc/webinar-reaction-progress-kinetic-analysis-0009.
(32) Wikipedia page: https://en.wikipedia.org/wiki/Reaction_progress_kinetic_analysis.
(33) Selected examples: (a) Devery, J. J.; Conrad, J. C.; MacMillan, D. W. C.; Flowers, R. A., II *Angew. Chem., Int. Ed.* **2010**, *49*, 6106. (b) Wagner, A. J.; Rychnovsky, S. D. *Org. Lett.* **2013**, *15*, 5504. (c) Scott, M.; Sud, A.; Boess, E.; Klussmann, M. *J. Org. Chem.* **2014**, *79*, 12033.

DOI: 10.1021/jacs.5b05841
J. Am. Chem. Soc. 2015, 137, 10852−10866